

ENOX2 NADH Oxidase: A BCR-ABL1-Dependent Cell Surface and Secreted Redox Protein in Chronic Myeloid Leukemia

ENOX2 NADH Oksidaz: Kronik Myeloid Lösemi'de Hücre Dışına Salgılanan ve BCR-ABL1-Bağımlı Hücre Yüzeyi Redoks Proteini

İ Seda Baykal^{1,2}, İ Maud Voldoire³, İ Christophe Desterke⁴, İ Nathalie Sorel⁵, İ Emilie Cayssials⁶, İ Hyacinthe Johnson-Ansah⁷, İ Agnes Guerci-Bresler⁸, İ Annelise Bennaceur-Griscelli⁹, İ Jean-Claude Chomeil¹⁰, İ Ali G. Turhan¹¹

¹İzmir Biomedicine and Genome Center, İzmir, Türkiye

²Dokuz Eylül University Faculty of Medicine, Department of Medical Biology, İzmir, Türkiye

³CHD La Roche-sur-Yon-Service de Médecine Onco-Hématologie, La Roche-sur-Yon, Pays de la Loire, France

⁴Université Paris-Saclay BU Kremlin-Bicêtre-Faculté de Médecine, Le Kremlin-Bicêtre, Île-de-France

⁵CHU Poitiers-Service de Cancérologie Biologique, Poitiers, France

⁶CHU Poitiers-Service d'Oncologie Hématologique et Thérapie Cellulaire, Poitiers, France

⁷CHRU de Caen-Service d'Hématologie Clinique, Caen, Basse-Normandie, France

⁸Hôpital Brabois-Service d'Hématologie Clinique, Vandoeuvre les Nancy, France

⁹AP-HP Université Paris Saclay-Service d'Hématologie, Le Kremlin-Bicêtre, Île-de-France, France

¹⁰INSERM-UA9, Villejuif, Paris, Île-de-France, France

¹¹Paris-Saclay University-Service d'hematologie, Hopital Bicetre, Paris, Villejuif, France

Abstract

Objective: Chronic myeloid leukemia (CML) is a disease caused by the acquisition of *BCR-ABL1* fusion in hematopoietic stem cells. In this study, we focus on the oncofetal ENOX2 protein as a potential secretable biomarker in CML.

Materials and Methods: We used cell culture, western blot, quantitative RT-PCR, ELISA, transcriptome analyses, and bioinformatics techniques to investigate *ENOX2* mRNA and protein expression.

Results: Western blot analyses of UT-7 and TET-inducible Ba/F3 cell lines demonstrated the upregulation of the ENOX2 protein. *BCR-ABL1* was found to induce ENOX2 overexpression in a kinase-dependent manner. We confirmed increased *ENOX2* mRNA expression in a cohort of CML patients at diagnosis. In a series of CML patients, ELISA assays showed a highly significant increase of *ENOX2* protein levels in the plasma of patients with CML compared to controls. Reanalyzing the transcriptomic dataset confirmed *ENOX2* mRNA overexpression in the chronic phase of the disease. Bioinformatic analyses identified several genes whose mRNA expressions were positively correlated with ENOX2 in the context of *BCR-ABL1*. Some of them encode proteins involved in cellular functions compatible with the growth deregulation observed in CML.

Conclusion: Our results highlight the upregulation of a secreted redox protein in a *BCR-ABL1*-dependent manner in CML. The data presented here suggest that ENOX2, through its transcriptional mechanism, plays a significant role in *BCR-ABL1* leukemogenesis.

Keywords: CML, ENOX2, Biomarker, Chronic myeloid leukemia, Redox protein, Secreted protein

Öz

Amaç: Kronik myeloid lösemi (KML), hematopoietik kök hücrelerde *BCR-ABL1* füzyon geninin ortaya çıkması ile oluşan bir hastalıktır. Bu çalışmada, KML'de potansiyel bir salgılanabilir biyobelirteç olan onkogen fetal ENOX2 proteinine odaklanılmıştır.

Gereç ve Yöntemler: *ENOX2* mRNA ve protein ekspresyonunu araştırması için hücre kültürü, Western blot, kantitatif RT-PCR, ELISA, transkriptom analizleri ve biyoinformatik teknikler kullanılmıştır.

Bulgular: UT-7 ve TET indüklenebilir Ba/F3 hücre hatlarında yapılan Western blot analizleri, ENOX2 proteininin ekspresyonunun arttığını göstermiştir. *BCR-ABL1*'in ENOX2 gen ifadesini kinaz bağımlı olarak artırdığı gösterilmiştir. KML diagnoz hastaları kohortunda *ENOX2* mRNA ekspresyonunun arttığı doğrulanmıştır. KML hastalarına ait kan örneklerinde yapılan ELISA testleri, KML hastalarının plazmalarında kontrol grubuna kıyasla *ENOX2* protein seviyelerinde anlamlı bir artış olduğunu göstermiştir. Transkriptomik veri setlerinin yeniden analiz edilmesiyle hastalığın kronik fazında *ENOX2* mRNA ekspresyonunun arttığı doğrulanmıştır. Biyoinformatik analizlerle, *BCR-ABL1* bağlamında ENOX2 ile pozitif korelasyon gösteren, KML'de gözlenen bölünme deregülasyonunda hücresel işlevlere katılan çeşitli genler tanımlanmıştır.

Sonuç: Bulgularımız KML'de *BCR-ABL1*-bağımlı şekilde salgılanan ENOX2 redoks proteininin ifadesinin arttığını göstermektedir. Burada sunulan veriler, *ENOX2*'nin transkripsiyonel mekanizması yoluyla *BCR-ABL1* lösemi oluşumunda önemli bir rol oynadığını göstermektedir.

Anahtar Sözcükler: ENOX2, KML, Kronik myeloid lösemi, Redoks proteini, Biyobelirteç, Salgı proteini



Introduction

Chronic myeloid leukemia (CML) therapy has been radically modified by tyrosine kinase inhibitors (TKIs). The life expectancy of patients diagnosed with chronic-phase CML (CP-CML) and responding to TKI therapy appears to be similar to that of the general population [1]. The BCR-ABL1 tyrosine kinase responsible for CML initiates uncontrolled granulocyte proliferation, decreased adhesion to the medullar niche, apoptosis inhibition, and genetic instability. Most aberrant signaling pathways downstream of *BCR-ABL1* have been known for a long time [2]. Using the human granulocyte macrophage colony-stimulating factor (GM-CSF)-dependent erythro/megakaryoblastic UT-7 cell line, our group previously uncovered novel nonconventional actors downstream of the BCR-ABL1 signaling [3,4].

In the present study, we highlight the upregulation of *ENOX2* (ecto-nicotinamide adenine dinucleotide oxidase disulfide thiol exchanger 2) in *BCR-ABL1*-positive cell lines. *ENOX2* is a growth-related cell surface protein that combines two oscillatory enzymatic activities, those of hydroquinone NADH oxidase and protein disulfide-thiol oxidoreductase, that alternate within a period of 22 minutes, generating an ultradian cellular biological clock of 22 hours (Supplementary Figure S1) [5,6]. The *ENOX2* protein is present during the embryonic period and almost entirely absent in normal adult cells, and it reappears in most cancer cells [7]. *ENOX2* proteins can be released from tumor cells into extracellular fluids, in which they can be detected [8].

In our experiments, increased *ENOX2* mRNA expression was also found in primary cells from patients with CP-CML at diagnosis. Using the UT-7 and inducible Ba/F3 cell lines, we confirmed *ENOX2* upregulation at the protein level and demonstrated that this phenomenon was linked to BCR-ABL1 tyrosine kinase activity. In addition, a significant increase in *ENOX2* protein levels was observed in the plasma of patients at the time of diagnosis. Reanalyzing a publicly available database, we found that *ENOX2* mRNA expression was characteristic of CP-CML.

Materials and Methods

UT-7 and TET-Inducible Ba/F3 Cell Lines

The human hematopoietic UT-7 parental cell line (UT-7/p) was kindly provided by Dr. Komatsu et al. [9]. Its counterparts transduced with either native BCR-ABL1-p210 (UT-7/11 cells) or T315I-mutated-*BCR-ABL1* (UT-7/T315I) resistant to first- and second-generation TKIs were previously characterized by our group [10,11]. The doxycycline-inducible BaF/p210 sin1.55 cell line was also previously described [12]. In this TET-OFF model, the addition of doxycycline in the cell culture medium turns off BCR-ABL1 expression.

Patients and Healthy Donors

For *ENOX2* mRNA expression analysis, 36 CP-CML patients were tested at diagnosis along with a cohort of 27 healthy control donors (Supplementary Table S1). Concerning the quantification of *ENOX2* protein in plasma samples, independent cohorts of 41 CP-CML patients at diagnosis and 28 healthy controls were also analyzed. This nonclinical study was approved by the INSERM UA9 Ethics Committee on February 11, 2014. All patients and healthy donors gave informed consent in accordance with the Declaration of Helsinki.

Transcriptome Experiments

Analyses were performed using UT-7/11 cells expressing BCR-ABL1 as compared to parental UT-7 cells. Total RNA was extracted from UT-7 cells. RNA quantification was performed with a NanoDrop device (Thermo Fisher Scientific, Santa Clara, CA, USA) and sample quality was evaluated with the Bioanalyzer-2100 instrument (Agilent Technologies, Santa Clara, CA, USA). Transcriptome analysis was performed on the Human Genome U133A Array version of the Affymetrix platform (Affymetrix, Santa Clara, CA, USA). The results of each experimental group were normalized with the RMA algorithm (Affymetrix).

Quantitative RT-PCR Assays

Total RNA from whole blood was reverse-transcribed using the High-Capacity cDNA Reverse Transcription Kit (Life Technologies, Foster City, CA, USA) and qRT-PCR experiments were performed using the 7900 Sequence Detection System (Life Technologies). TaqMan pre-developed assay reagents were used to quantify *ENOX2* (Hs00197268_m1) and *B2M* as an internal reference (beta-2 microglobulin, Hs00187842_m1). The Hs00197268_m1 TaqMan expression assay allows the detection of all *ENOX2* mRNA splicing variants (Supplementary Figure S2). PCR reactions were prepared in duplicate using TaqMan Universal PCR Master Mix (Life Technologies) and *ENOX2/B2M* ratios were determined using the ΔCt method.

Western Blotting

The proteins were quantified by BCA assay, separated by polyacrylamide gel electrophoresis, and wet-transferred to PVDF membranes. Membranes were probed with specific primary and HRP-conjugated secondary antibodies and revealed by chemiluminescence with SuperSignal West Dura or Femto reagents. Data were acquired using the G-BOX-iChemi Image Capture system (Syngene, Frederick, MD, USA). The antibodies used were as follows: anti-*ENOX2* (LS-C346209, LifeSpan BioSciences, Seattle, WA, USA) and anti-ABL1 (Santa Cruz Biotechnology) for the detection of translocated and non-translocated ABL1 protein, and anti-beta-actin (Sigma-Aldrich) with dilution as recommended by the manufacturer.

ENOX2 Protein Concentration in Blood Plasma

ENOX2 protein in blood plasma was quantified using the human Ecto-NOX Disulfide-Thiol Exchanger 2 ELISA Kit (MBS 943476, MyBioSource Inc., San Diego, CA, USA) according to the manufacturer's guidelines.

Transcriptome Dataset GSE4170

Using a DNA microarray, Radich et al. [13] aimed to compare gene expression between the chronic (<10% blasts), accelerated (10%-30% blasts), and blast phase (>30% blasts) by analyzing 91 cases of CML using normal immature CD34+ cells as a reference. The Rosetta/Merck Human 25k v2.2.1 data matrix of normalized log-ratios from GSE4170 was downloaded from the Gene Expression Omnibus (GEO) website and annotated with the GPL2029 annotation platform to be reanalyzed, focusing on *ENOX2* mRNA expression.

Bioinformatics Microarray Data Analysis

Genes whose expressions were significantly correlated with the expression of *ENOX2* during CML progression were determined from the transcriptomes of hematopoietic cells from the GEO GSE4170 dataset with the Pavlidis template matching algorithm. During this analysis, taking *ENOX2* expression as the outcome, the thresholds of a positive Pearson correlation coefficient greater than 0.80 and a p-value less than 1.E-6 were used to define significant genes with positive correlations to *ENOX2* expression during the progression of CML [14]. These significant genes were retained to draw an expression heatmap associated with a parallel coordinate plot obtained with the MADE4 [15] and GGally R packages, respectively. Gene clustering on the expression heatmap was done with Pearson correlation distances. The expression profile correlating with *ENOX2* in CML cells was used to generate functional enrichment with Go-Elite Standalone software version 1.2 in the Gene Ontology Biological Process database including the *Homo sapiens* EnsMart77Plus (Ensembl - Biomart) update [16]. Unsupervised principal component analysis was performed on the correlated gene expression profile with the FactoMiner R package. The p-values were calculated by group discrimination on the first principal component axis. The functional interaction network was built with functional relations identified during enrichment analysis with Cytoscape software version 3.2.1 [17].

Scatter Dot Plots, Boxplots, and Statistical Analysis

Data on *ENOX2* gene expression or protein concentrations in plasma were expressed as scatter dot plots or boxplots with medians (Prism version 8.0, GraphPad Software, San Diego, CA, USA). The two-sided Welch t-test was used to determine statistical significance between data groups. Differences were considered significant at $p < 0.05$.

Results

ENOX2 Is Overexpressed in BCR-ABL1-Expressing UT-7 Cell Lines

We performed a transcriptome assay to identify genes up- or downregulated in *BCR-ABL1*-expressing UT-7 cells. To this end, we compared the UT-7/11 cells (n=3), which expressed high levels of BCR-ABL1 protein, to parental UT-7 cells (UT7/p, n=3). We focused on *ENOX2* mRNA, which was not previously known to be overexpressed in *BCR-ABL1*-positive leukemia. As shown in Figure 1A, *ENOX2* was significantly upregulated (x2.4, $p=0.0012$) in the UT-7/11 cells.

BCR-ABL1 Induces the Production of ENOX2 Protein in BCR-ABL1-Expressing Cell Lines

Parental UT-7, UT-7/11, and UT-7/T315I cells were used to analyze the presence of *ENOX2* protein by western blot. Figure 1B confirms the presence of BCR-ABL1 protein in UT-7/11 and UT-7/T315I cells in contrast to parental UT-7 cells. Concerning *ENOX2*, high protein levels were produced in the BCR-ABL1-expressing UT-7 cell line (native UT-7/11 and mutated-UT-7/T315I) compared to UT-7/p control cells (Figure 1C).

To ensure that *ENOX2* overexpression would be related to the presence of *BCR-ABL1*, we used a Ba/F3 cell line transduced with *BCR-ABL1* under the control of the TET promoter (BaF/p210 sin1.55). This inducible model was appropriate insofar as the BCR-ABL1 protein was inhibited by doxycycline (Figure 1D). Decreased *ENOX2* protein expression was observed in response to doxycycline added to the culture medium (Figure 1E). *BCR-ABL1* and *ENOX2* were re-expressed on day 12 upon washing out the doxycycline from the cell medium (Figures 1D and 1E). Consequently, *ENOX2* overexpression appeared to be related to the presence of *BCR-ABL1* insofar as inhibition of *BCR-ABL1* expression in the TET-inducible Ba/F3 model led to a reduction in *ENOX2* protein synthesis.

We then asked whether the expression of *ENOX2* in CML cells was a tyrosine kinase-dependent event. Western blot experiments showed that *ENOX2* protein expression was reduced in the UT7/11 cells treated with imatinib at 1 μ M for 6, 18, and 24 hours (Figure 2A). The same experiments performed on the UT-7/p cell line showed no modification of basal *ENOX2* expression (Figure 2B).

ENOX2 mRNA Expression Is Increased in Primary Cells from Patients at Diagnosis

To validate the results obtained for *BCR-ABL1*-expressing cells, we examined *ENOX2* mRNA expression by qRT-PCR in blood samples obtained from a cohort of CP-CML patients at diagnosis. *ENOX2* mRNA levels were significantly increased in samples obtained from patients with CP-CML at diagnosis ($p < 0.0001$) compared to healthy donors with a fold change of 4.75 (Figure 3A). We did not find any correlations between *ENOX2* mRNA expression and

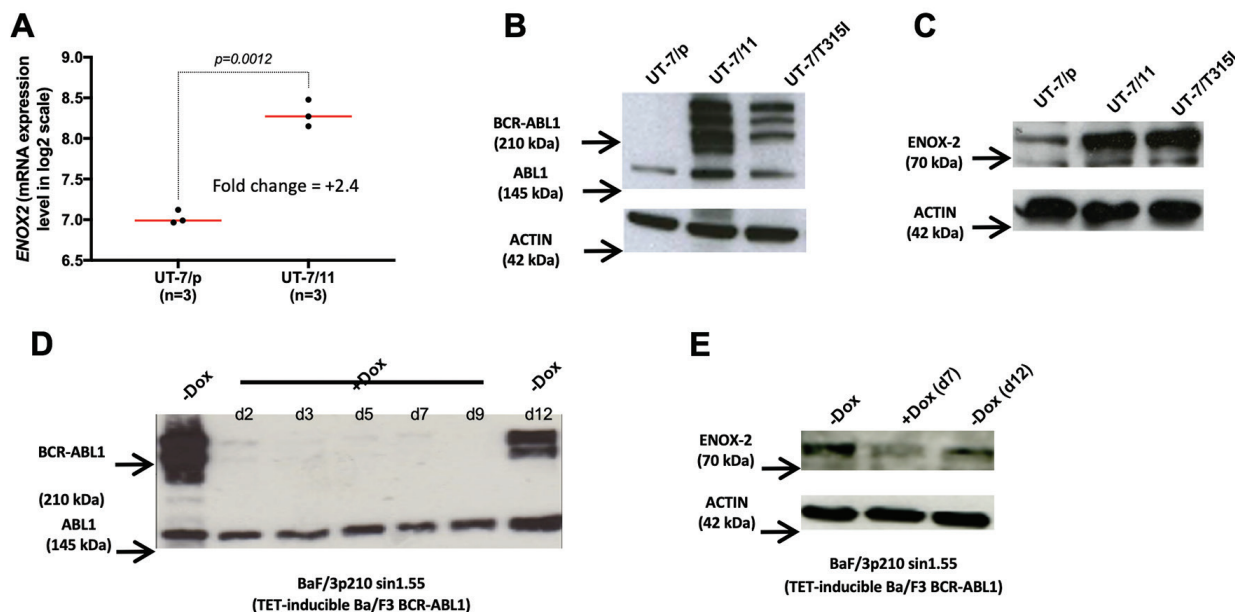


Figure 1. ENOX2 is upregulated by BCR-ABL1 in UT-7/11 and TET-inducible Ba/F3 cell lines. **A:** mRNA expression in UT-7/11 (transfected by *BCR-ABL1*) compared with UT-7/Parental. **B, C, D, E:** Western blot analyses of BCR-ABL and ENOX-2 protein in UT-7 cell lines and TET-inducible Ba/F3 cell line.

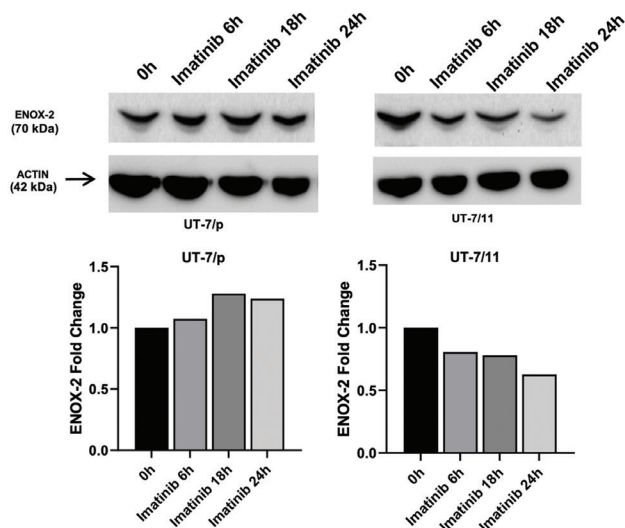


Figure 2. ENOX2 protein upregulation depends on the BCR-ABL1 tyrosine kinase-activity. **A:** Western blot analysis performed with the UT-7/11 cell line under tyrosine kinase inhibition conditions (imatinib at 1 μ M for 6, 18, and 24 hours) showed the reduction of ENOX2 protein expression. **B:** Western blot analysis performed with the UT-7/p cell line as a control.

Sokal scores or patient outcomes in this cohort.

ENOX2 Protein Levels Are Significantly Increased in the Plasma of CML Patients

We determined ENOX2 protein concentrations in the plasma of patients with CML at diagnosis compared to healthy controls using an ELISA method. A significant increase in plasma ENOX2 protein levels ($p < 0.0001$) was shown in CP-CML patients at diagnosis before TKI therapy (Figure 3B). The extended frequency

distribution of ENOX2 protein levels was undoubtedly due to heterogeneity between patients. Furthermore, no correlation was found between ENOX2 protein levels in the plasma and white blood cell count at diagnosis (Supplementary Figure S3).

ENOX2 mRNA Overexpression Is Characteristic of the Chronic Phase of CML

We reanalyzed a publicly available transcriptome dataset from CML patients during different phases of the disease (GSE4170). *ENOX2* mRNA expression data were retrieved from the GEO database and analyzed independently. *ENOX2* mRNA upregulation (using normal immature CD34+ cells as the reference) was observed in this independent study for all CP-CML patients (Figure 3C). In addition, *ENOX2* expression in the accelerated and blast phases was comparable to that of normal CD34+ cells and appeared to be heterogeneous.

mRNA Expressions of ENOX2 and Related Genes Distinguish the Chronic Phase of CML from Advanced Phases

Exploiting the GSE4170 transcriptome dataset, we next tried to discover genes positively correlated with *ENOX2* mRNA expression. The Pavlidis template matching algorithm used with *ENOX2* as a predictor highlighted 301 related genes with a positive r correlation coefficient greater than 0.80 and a p -value threshold less than $p < 1E-6$ (Supplementary Table S2). The high correlation with *ENOX2* mRNA expression is illustrated for eight potentially relevant protein-coding genes in Supplementary Figure S4. The heatmap and parallel coordinate plot revealed that the high mRNA expression levels of these 301 genes were characteristic of the CP-CML (Figure 4A). Unsupervised principal

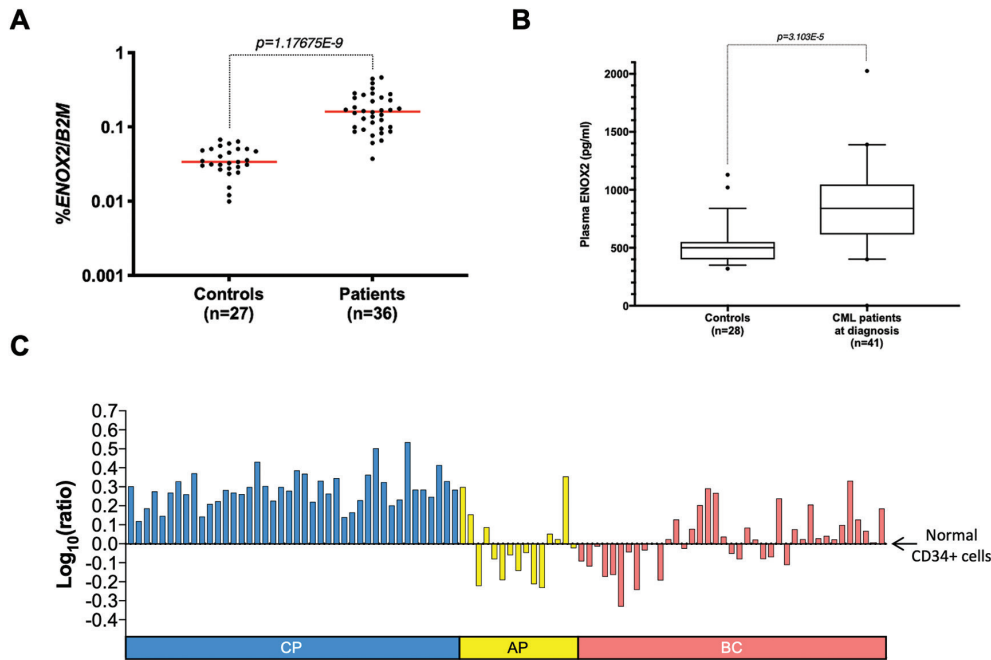


Figure 3. ENOX2 is overexpressed in primary cells from patients with chronic-phase chronic myeloid leukemia (CP-CML). **A:** Scatter dot plot analyses of *ENOX2* mRNA expression of CML patients at diagnosis. **B:** Boxplot shows high ENOX2 protein in plasma levels of CP-CML patients at diagnosis. **C:** GSE4170 GEO dataset reanalysis. *ENOX2* mRNA relative expressions in CML cells corresponding to patients in the chronic phase (CP), acute phase (AP), and blast phase (BC) compared to normal immature CD34+ cells.

component analysis performed with the *ENOX2* pattern matching gene expression profile allowed highly significant discrimination of the chronic phase from the accelerated and blastic phases (Figure 4B, $p < 0.0001$).

Several Proteins of a Potential ENOX2 Network May Be Involved in Crucial Biological Processes

Functional enrichment performed with the *ENOX2* pattern matching in the Gene Ontology Biological Process database emphasized 49 genes out of 301 involved in essential cell processes (Figure 4C). In the context of *ENOX2* mRNA overexpression in CP-CML, several major biological functions appear to be activated: angiogenesis, NOTCH signaling, cell morphogenesis differentiation, circadian rhythm, RAS signaling, cell proliferation, G-protein receptor pathways, integrin-mediated signaling, carbohydrate homeostasis, stress-activated protein kinase, and RHO GTPase activities (Figure 4D, Supplementary Table S3).

Discussion

The involvement of *ENOX2* in *BCR-ABL1*-positive leukemias has yet to be shown. Here, we have established that *ENOX2* mRNA was overexpressed in both experimental models of *BCR-ABL1*-induced cell transformation and primary leukemic cells from newly diagnosed CP-CML patients. Western blots analyses confirmed the presence of higher levels of ENOX2 protein in *BCR-ABL1*-expressing murine and human cell lines.

This overexpression is directly influenced by the presence of the *BCR-ABL1* oncoprotein and related to its constitutive tyrosine kinase activity. We also observed a significant increase in plasma ENOX2 levels in CML patients at diagnosis. Reanalyzing a transcriptomic dataset from a previously reported gene profiling study [13], we observed that *ENOX2* mRNA expression is restricted to the chronic phase of the disease. Nevertheless, we could not determine here whether ENOX2 is a direct or an indirect target of *BCR-ABL1*.

The *ENOX2* gene is only translated during early embryogenesis and cancer development. Therefore, the physiological function of ENOX2 appears to be restricted to the embryonic period [7], in which this oncofetal protein located at the plasma membrane has oscillating enzymatic activity. Little is known about the reappearance and oncogenic function of ENOX2 in adult cells. However, it has been shown that ENOX2 proteins are constitutively activated in cancers and could promote cell proliferation [18,19]. As they are not firmly anchored into the cell membrane, ENOX2 proteins can be shed into extracellular fluids. This circulating form has been detected in the sera of patients suffering from various tumors [20], whereas it is present only at very low levels in healthy subjects [21]. In the present study, significant levels of circulating ENOX2 protein detected in plasma from CP-CML patients at diagnosis are consistent with the prior data.

In silico reanalysis suggested that the mRNA expressions of several genes are positively correlated with *ENOX2* expression in

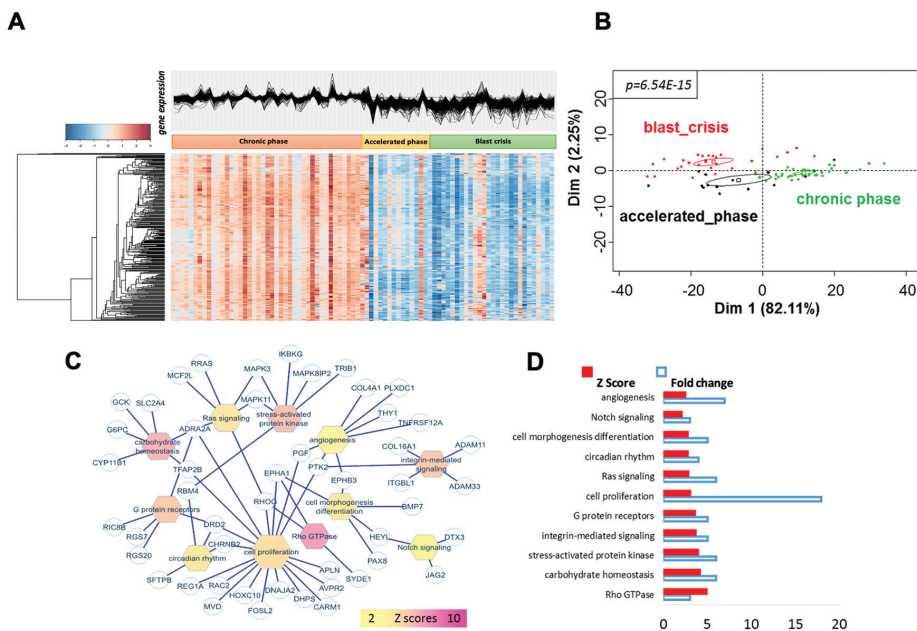


Figure 4. A potential network correlated with *ENOX2* gene expression in patients with chronic-phase chronic myeloid leukemia (CP-CML) is highlighted. **A:** Heatmap and parallel coordinate plot revealed 301 genes positively correlated with *ENOX2* mRNA expression. **B:** Unsupervised principal component analysis performed with *ENOX2* pattern matching gene expression profile distinguished the chronic phase of CML from the accelerated and blast phases. Correlation p-values were evaluated for phase discrimination on the first principal axis; ellipses around the barycenter were estimated with 75% confidence. **C:** Functional enrichment performed with *ENOX2* pattern matching in the Gene Ontology Biological Process database revealed 49 genes involved in essential cellular processes. Results are presented as a Cytoscape network view showing both biological functions and related genes. The color of nodes in the network is relative to the Z scores obtained during functional enrichment. The size of function nodes is relative to the number of genes enriched in the corresponding function mapped on the network. **D:** Bar plots represent both Z scores and gene expression fold changes for the different molecular functions defined by the Gene Ontology Biological Process database.

the context of BCR-ABL1, thereby highlighting critical biological functions. These results for a substantial number of individual genes are highly significant, and it is quite unlikely that all of these genes are not translated into functional proteins. Consequently, high *ENOX2* mRNA expression probably goes along with the activation of cell proliferation and differentiation through genes encoding proteins from different pathways. *ENOX2* overexpression has been linked to cell proliferation, migration, and increased expression of mesenchymal markers in some cancers [22]. Interestingly, these data are in line with the characteristics of CML dysregulation [23]. Among the genes found to be positively correlated with *ENOX2* mRNA expression in a CML context, some have already been confirmed to be involved in BCR-ABL1-mediated leukemogenesis. This is the case for RAC2 GTPases, ERK MAP-kinase, FAK (focal adhesion kinase), NOTCH1, and PIGF (placental growth factor) [24,25,26,27,28].

In addition to this potential biological feature, we wondered whether *ENOX2* could be a surrogate marker or even a therapeutic target. Based on our experiments, we can state that *ENOX2* is the first secreted biomarker described in CML. On the other hand, we did not find any relationship between *ENOX2* mRNA expression or *ENOX2* plasma levels and the clinical course or the most relevant biological parameters. Some antioxidant agents

(capsaicin, omega-3 polyunsaturated fatty acids, or synthetic isoflavone) could exert antitumor effects by inhibiting *ENOX2* enzymatic activity [29,30]. All of these agents could represent a potential *ENOX2*-targeted therapy for malignant diseases. In CML, the majority of patients treated with TKIs achieve a sustained molecular response. However, two circumstances may require other therapeutic options: the complete resistance to all available TKIs and the persistence of quiescent leukemic stem cells. The potential value of *ENOX2* as a druggable target in these contexts warrants further exploration.

Conclusion

Overall, we propose that *BCR-ABL1* upregulates *ENOX2* in the chronic phase of CML. To the best of our knowledge, the association between the reactivation of *ENOX2* in adult cells and deregulated tyrosine kinase activity was never previously observed. Our results suggest that *ENOX2* could play a role in the pathogenesis of CML in a BCR-ABL1-dependent manner. Further studies are required to clarify the link between BCR-ABL1 and *ENOX2*.

Ethics

Ethics Committee Approval: This non-clinical study was approved by the INSERM UA9 Ethics Committee on February 11, 2014.

Informed Consent: All patients and healthy donors gave informed consent in accordance with the Declaration of Helsinki.

Authorship Contributions

Concept: S.B., M.V., C.D., N.S., E.C., H.J-A., A.G-B., A.B-G., J.C-C., A.G.T.; Design: S.B., M.V., C.D., N.S., E.C., H.J-A., A.G-B., A.B-G., J.C-C., A.G.T.; Data Collection or Processing: S.B., M.V., C.D., N.S., E.C., H.J-A., A.G-B., A.B-G., J.C-C., A.G.T.; Analysis or Interpretation: S.B., M.V., C.D., N.S., E.C., H.J-A., A.G-B., A.B-G., J.C-C., A.G.T.; Literature Search: S.B., M.V., C.D., N.S., E.C., H.J-A., A.G-B., A.B-G., J.C-C., A.G.T.; Writing: S.B., M.V., C.D., N.S., E.C., H.J-A., A.G-B., A.B-G., J.C-C., A.G.T.

Conflict of Interest: No conflict of interest was declared by the authors.

Financial Disclosure: The authors declared that this study received no financial support.

References

- Bower H, Björkholm M, Dickman PW, Höglund M, Lambert PC, Andersson TM. Life expectancy of patients with chronic myeloid leukemia approaches the life expectancy of the general population. *J Clin Oncol* 2016;34:2851-2857.
- Cilloni D, Saglio G. Molecular pathways: BCR-ABL. *Clin Cancer Res* 2012;18:930-937.
- Girerd S, Tosca L, Herault O, Vignon C, Biard D, Aggoune D, Dkhissi F, Bonnet ML, Sorel N, Desterke C, Bennaceur-GrisCELLI A, Tachdjian G, Guilhot F, Guilhot J, Chomel JC, Turhan AG. Superoxide dismutase 2 (SOD2) contributes to genetic stability of native and T315I-mutated BCR-ABL expressing leukemic cells. *Biochem Biophys Res Commun* 2018;498:715-722.
- Desterke C, Voltaire M, Bonnet ML, Sorel N, Pagliaro S, Rahban H, Bennaceur-GrisCELLI A, Cayssials E, Chomel JC, Turhan AG. Experimental and integrative analyses identify an ETS1 network downstream of BCR-ABL in chronic myeloid leukemia (CML). *Exp Hematol* 2018;64:71-83.e8.
- Chueh PJ, Kim C, Cho N, Morr  DM, Morr  DJ. Molecular cloning and characterization of a tumor-associated, growth-related, and time-keeping hydroquinone (NADH) oxidase (tNOX) of the HeLa cell surface. *Biochemistry* 2002;41:3732-3741.
- Morr  DJ, Chueh PJ, Pletcher J, Tang X, Wu LY, Morr  DM. Biochemical basis for the biological clock. *Biochemistry* 2002;41:11941-11945.
- Cho N, Morr  DJ. Early developmental expression of a normally tumor-associated and drug-inhibited cell surface-located NADH oxidase (ENOX2) in non-cancer cells. *Cancer Immunol Immunother* 2009;58:547-552.
- Morr  DJ, Hostetler B, Taggart DJ, Morr  DM, Musk AW, Robinson BW, Creaney J. ENOX2-based early detection (ONCOblot) of asbestos-induced malignant mesothelioma 4-10 years in advance of clinical symptoms. *Clin Proteomics* 2016;13:2.
- Komatsu N, Nakauchi H, Miwa A, Ishihara T, Eguchi M, Moroi M, Okada M, Sato Y, Wada H, Yawata Y, Suda T, Miura Y. Establishment and characterization of a human leukemic cell line with megakaryocytic features: dependency on granulocyte-macrophage colony-stimulating factor, interleukin 3, or erythropoietin for growth and survival. *Cancer Res* 1991;51:341-348.
- Issaad C, Ahmed M, Novault S, Bonnet ML, Bennardo T, Varet B, Vainchenker W, Turhan AG. Biological effects induced by variable levels of BCR-ABL protein in the pluripotent hematopoietic cell line UT-7. *Leukemia* 2000;14:662-670.
- Aggoune D, Tosca L, Sorel N, Bonnet ML, Dkhissi F, Tachdjian G, Bennaceur-GrisCELLI A, Chomel JC, Turhan AG. Modeling the influence of stromal microenvironment in the selection of ENU-induced BCR-ABL1 mutants by tyrosine kinase inhibitors. *Oncoscience* 2014;1:57-68.
- Dugray A, Geay JF, Foudi A, Bonnet ML, Vainchenker W, Wendling F, Louache F, Turhan AG. Rapid generation of a tetracycline-inducible BCR-ABL defective retrovirus using a single autoregulatory retroviral cassette. *Leukemia* 2001;15:1658-1662.
- Radich JP, Dai H, Mao M, Oehler V, Schelter J, Druker B, Sawyers C, Shah N, Stock W, Willman CL, Friend S, Linsley PS. Gene expression changes associated with progression and response in chronic myeloid leukemia. *Proc Natl Acad Sci U S A* 2006;103:2794-2799.
- Pavlidis P, Noble WS. Analysis of strain and regional variation in gene expression in mouse brain. *Genome Biol* 2001;2:RESEARCH0042.
- Culhane AC, Thioulouse J, Perri re G, Higgins DG. MADE4: An R package for multivariate analysis of gene expression data. *Bioinformatics* 2005;21:2789-2790.
- Zambon AC, Gaj S, Ho I, Hanspers K, Vranizan K, Evelo CT, Conklin BR, Pico AR, Salomonis N. GO-Elite: a flexible solution for pathway and ontology over-representation. *Bioinformatics* 2012;28:2209-2210.
- Cline MS, Smoot M, Cerami E, Kuchinsky A, Landys N, Workman C, Christmas R, Avila-Campilo I, Creech M, Gross B, Hanspers K, Isserlin R, Kelley R, Killcoyne S, Lotia S, Maere S, Morris J, Ono K, Pavlovic V, Pico AR, Vailaya A, Wang PL, Adler A, Conklin BR, Hood L, Kuiper M, Sander C, Schmulevich I, Schwikowski B, Warner GJ, Ideker T, Bader GD. Integration of biological networks and gene expression data using Cytoscape. *Nat Protoc* 2007;2:2366-2382.
- Bruno M, Brightman AO, Lawrence J, Werderitsh D, Morr  DM, Morr  DJ. Stimulation of NADH oxidase activity from rat liver plasma membranes by growth factors and hormones is decreased or absent with hepatoma plasma membranes. *Biochem J* 1992;284(Pt 3):625-628.
- Yagiz K, Snyder PW, Morr  DJ, Morr  DM. Cell size increased in tissues from transgenic mice overexpressing a cell surface growth-related and cancer-specific hydroquinone oxidase, tNOX, with protein disulfide-thiol interchange activity. *J Cell Biochem* 2008;105:1437-1442.
- Hostetler B, Weston N, Kim C, Morr  DM, Morr  DJ. Cancer site-specific isoforms of ENOX2 (tNOX), a cancer-specific cell surface oxidase. *Clin Proteomics* 2009;5:46-51.
- Morr  DJ, Hostetler B, Weston N, Kim C, Morr  DM. Cancer type-specific tNOX isoforms: a putative family of redox protein splice variants with cancer diagnostic and prognostic potential. *Biofactors* 2008;34:201-207.
- Zeng ZM, Chuang SM, Chang TC, Hong CW, Chou JC, Yang JJ, Chueh PJ. Phosphorylation of serine-504 of tNOX (ENOX2) modulates cell proliferation and migration in cancer cells. *Exp Cell Res* 2012;318:1759-1766.
- Clarkson BD, Strife A, Wisniewski D, Lambek C, Carpino N. New understanding of the pathogenesis of CML: a prototype of early neoplasia. *Leukemia* 1997;11:1404-1428.
- Thomas EK, Cancelas JA, Zheng Y, Williams DA. Rac GTPases as key regulators of p210-BCR-ABL-dependent leukemogenesis. *Leukemia* 2008;22:898-904.
- Woessmann W, Mivechi NF. Role of ERK activation in growth and erythroid differentiation of K562 cells. *Exp Cell Res* 2001;264:193-200.
- Le Y, Xu L, Lu J, Fang J, Nardi V, Chai L, Silberstein LE. FAK silencing inhibits leukemogenesis in BCR/ABL-transformed hematopoietic cells. *Am J Hematol* 2009;84:273-278.
- Aljedai A, Buckle AM, Hiwarkar P, Syed F. Potential role of Notch signalling in CD34+ chronic myeloid leukaemia cells: cross-talk between Notch and BCR-ABL. *PLoS One* 2015;10:e0123016.

28. Schmidt T, Kharabi Masouleh B, Loges S, Cauwenberghs S, Fraisl P, Maes C, Jonckx B, De Keersmaecker K, Kleppe M, Tjwa M, Schenk T, Vinckier S, Fragoso R, De Mol M, Beel K, Dias S, Verfaillie C, Clark RE, Brümmendorf TH, Vandenberghe P, Rafii S, Holyoake T, Hochhaus A, Cools J, Karin M, Carmeliet G, Dewerchin M, Carmeliet P. Loss or inhibition of stromal-derived PIGF prolongs survival of mice with imatinib-resistant Bcr-Abl1+ leukemia. *Cancer Cell* 2011;19:740-753.
29. Morre J, Morrè DM, Brightmore R. Omega-3 but not omega-6 unsaturated fatty acids inhibit the cancer-specific ENOX2 of the HeLa cell surface with no effect on the constitutive ENOX1. *J Diet Suppl* 2010;7:154-158.
30. Morrè DJ, Korty T, Meadows C, Ades LM, Morrè DM. ENOX2 target for the anticancer isoflavone ME-143. *Oncol Res* 2014;22:1-12.

Supplementary Table S1. Patients' characteristics in the cohort for <i>ENOX2</i> mRNA expression.								
Patient			Molecular follow-up (% <i>BCR-ABL1/ABL1S</i>)		TKI discontinuation			
No.	Sex	Age at diagnosis (years)	Last test (years following diagnosis)	Molecular response	Yes/no	Time to cessation (years following diagnosis)	Result	Duration of TFS (years)
1	M	55.2	11.9	MR5	Yes	4.1	TFS	7.8
2	M	60.1	3.0	MR3	No			
3	F	45.2	12.6	MR4.5	Yes	6.5	TFS	6.1
4	M	76.2	7.9	MR4.5	No			
5	M	45.5	9.2	MR4.5	No			
6	F	43.7	12.0	MR5	Yes	5.6	TFS	6.4
7	M	66.9	1.8	MR3	No			
8	M	56.5	14.6	MR5	Yes	8.1	TFS	6.4
9	F	54.3	11.3	MR5	Yes	5.7	TFS	5.6
10	F	48.6	11.1	MR5	No			
11	F	60.4	15.0	MR2	No			
12	M	37.4	11.3	MR5	Yes	4.1	Recurrence	
13	M	58.5	8.2	MR4.5	No			
14	M	64.2	15.4	MR5	No			
15	M	60.5	15.3	MR3	Yes	7.5	Recurrence	
16	M	21.5	12.3	MR4.5	No			
17	F	56.8	11.3	MR5	Yes	8.0	Recurrence	
18	M	71.0	15.4	MR5	Yes	3.3	Recurrence	
19	F	34.9	17.4	MR3	No			
20	F	84.8	7.5	MR2	Yes	6.3	Recurrence	
21	M	48.6	13.3	MR4.5	Yes	7.9	TFS	5.3
22	F	57.9	5.6	MR4.5	No			
23	M	73.6	4.3	MR3	No			
24	M	69.6	4.4	MR4.5	No			
25	M	72.3	14.7	MR5	Yes	4.5	Recurrence	
26	M	64.8	11.6	MR4	No			
27	F	45.7	13.1	MR5	Yes	2.7	TFS	10.4
28	M	58.8	9.0	MR3	No			
29	M	74.4	11.1	MR4	No			
30	M	56.8	6.4	MR4.5	Yes	5.0	Recurrence	
31	F	40.3	13.7	MR5	No			
32	M	50.9	13.2	MR4	No			
33	M	83.8	4.9	MR4.5	No			
34	M	76.6	4.0	MR4	No			
35	M	59.3	17.0	MR4	Yes	10.7	Recurrence	
36	F	84.4	2.9	MR3	No			

TKI: Tyrosine kinase inhibitor; TFS: treatment-free remission. Molecular recurrence ("recurrence" in the table) is defined by the loss of major molecular response (MMR) or MR3. Molecular responses: MR2, %*BCR-ABL1/ABL1^S* <1%; MR3, %*BCR-ABL1/ABL1^S* <0.1%; MR4, %*BCR-ABL1/ABL1^F* <0.01%; MR4.5, %*BCR-ABL1/ABL1^F* <0.0032% (or 100000 copies > *ABL1* >32000 copies if undetectable *BCR-ABL1*); MR5, %*BCR-ABL1/ABL1^S* <0.001% (or *ABL1* >100000 copies if undetectable *BCR-ABL1*).

Supplementary Table S2. Genes correlated with ENOX2 mRNA expression. Genes known to be involved in essential cell processes are given in red.

Gene symbol	R value	p-value	Gene symbol	R value	p-value
<i>ENOX2</i>	1	<1.0e-6	<i>C11orf30</i>	0.88709366	<1.0e-6
<i>RCVRN</i>	0.96617126	<1.0e-6	<i>YIF1A</i>	0.8868629	<1.0e-6
<i>MYH11</i>	0.956953	<1.0e-6	<i>MAPK11</i>	0.8868171	<1.0e-6
<i>ANP32C</i>	0.9553184	<1.0e-6	<i>APLNR</i>	0.8862749	<1.0e-6
<i>EFEMP1</i>	0.9547916	<1.0e-6	<i>SSTR4</i>	0.88561755	<1.0e-6
<i>KLHDC8A</i>	0.9460578	<1.0e-6	<i>PCIF1</i>	0.88367957	<1.0e-6
<i>PTK2</i>	0.94451255	<1.0e-6	<i>OAZ1</i>	0.88326156	<1.0e-6
<i>APIP</i>	0.94312906	<1.0e-6	<i>C10orf116</i>	0.88301235	<1.0e-6
<i>POU3F4</i>	0.9411655	<1.0e-6	<i>APOA2</i>	0.8816541	<1.0e-6
<i>DISP1</i>	0.94022304	<1.0e-6	<i>CACYBP</i>	0.88127524	<1.0e-6
<i>ST7L</i>	0.936308	<1.0e-6	<i>PNMA3</i>	0.8805079	<1.0e-6
<i>FLJ32658</i>	0.93621475	<1.0e-6	<i>FRMPD1</i>	0.8795783	<1.0e-6
<i>JAG2</i>	0.9286973	<1.0e-6	<i>B4GALT7</i>	0.8795142	<1.0e-6
<i>ADAM6</i>	0.92834216	<1.0e-6	<i>RTBDN</i>	0.8791431	<1.0e-6
<i>ABCF3</i>	0.92229617	<1.0e-6	<i>CKAP2L</i>	0.87891597	<1.0e-6
<i>SYT17</i>	0.9192649	<1.0e-6	<i>BMP7</i>	0.87850946	<1.0e-6
<i>C10orf10</i>	0.91603184	<1.0e-6	<i>ODZ1</i>	0.8784246	<1.0e-6
<i>PCDHB6</i>	0.913041	<1.0e-6	<i>PPP5C</i>	0.8771678	<1.0e-6
<i>MPZL2</i>	0.9122278	<1.0e-6	<i>ECEL1</i>	0.8770625	<1.0e-6
<i>RPP14</i>	0.9114203	<1.0e-6	<i>HOXC10</i>	0.87696546	<1.0e-6
<i>OTOF</i>	0.9107501	<1.0e-6	<i>CACNA1H</i>	0.8764651	<1.0e-6
<i>NEUROG3</i>	0.90937275	<1.0e-6	<i>TACR2</i>	0.8759702	<1.0e-6
<i>TRIB1</i>	0.9091573	<1.0e-6	<i>GTF3C1</i>	0.8758702	<1.0e-6
<i>VPS45</i>	0.9077846	<1.0e-6	<i>SLC7A8</i>	0.8753778	<1.0e-6
<i>NAGS</i>	0.9065467	<1.0e-6	<i>DHPS</i>	0.8748936	<1.0e-6
<i>TNFRSF6B</i>	0.9064349	<1.0e-6	<i>MAGEA5</i>	0.8733235	<1.0e-6
<i>TJP3</i>	0.9064074	<1.0e-6	<i>TFAP2B</i>	0.8719522	<1.0e-6
<i>CPLX2</i>	0.9041828	<1.0e-6	<i>FAM65A</i>	0.87178475	<1.0e-6
<i>DMPK</i>	0.90411955	<1.0e-6	<i>KRT8</i>	0.87152994	<1.0e-6
<i>AP1M1</i>	0.9030762	<1.0e-6	<i>EPHB3</i>	0.87142307	<1.0e-6
<i>KIAA1244</i>	0.9018462	<1.0e-6	<i>REG3A</i>	0.87110436	<1.0e-6
<i>UTF1</i>	0.9012463	<1.0e-6	<i>SFTPA1B</i>	0.8706763	<1.0e-6
<i>NFATC4</i>	0.90038896	<1.0e-6	<i>NOTUM</i>	0.86875397	<1.0e-6
<i>RGS7</i>	0.899976	<1.0e-6	<i>PITX3</i>	0.86821973	<1.0e-6
<i>NRGN</i>	0.8981791	<1.0e-6	<i>LY6G6C</i>	0.8674368	<1.0e-6
<i>PTPRS</i>	0.898072	<1.0e-6	<i>ATN1</i>	0.8672403	<1.0e-6
<i>CRMP1</i>	0.8973751	<1.0e-6	<i>GGT1</i>	0.8672297	<1.0e-6
<i>ZNF107</i>	0.89688665	<1.0e-6	<i>SLC2A4</i>	0.8656502	<1.0e-6
<i>DTX3</i>	0.8961144	<1.0e-6	<i>CLDN4</i>	0.8652593	<1.0e-6
<i>GPX7</i>	0.8958358	<1.0e-6	<i>TPM2</i>	0.86410105	<1.0e-6
<i>GRIA1</i>	0.89445287	<1.0e-6	<i>CRAT</i>	0.8638945	<1.0e-6
<i>PAK4</i>	0.8937744	<1.0e-6	<i>PGF</i>	0.86375177	<1.0e-6
<i>LOC284701</i>	0.8899431	<1.0e-6	<i>PLXDC1</i>	0.8631661	<1.0e-6
<i>GPR17</i>	0.8890001	<1.0e-6	<i>DIS3</i>	0.862996	<1.0e-6
<i>PRPH</i>	0.8873445	<1.0e-6	<i>ATP1B2</i>	0.8626277	<1.0e-6

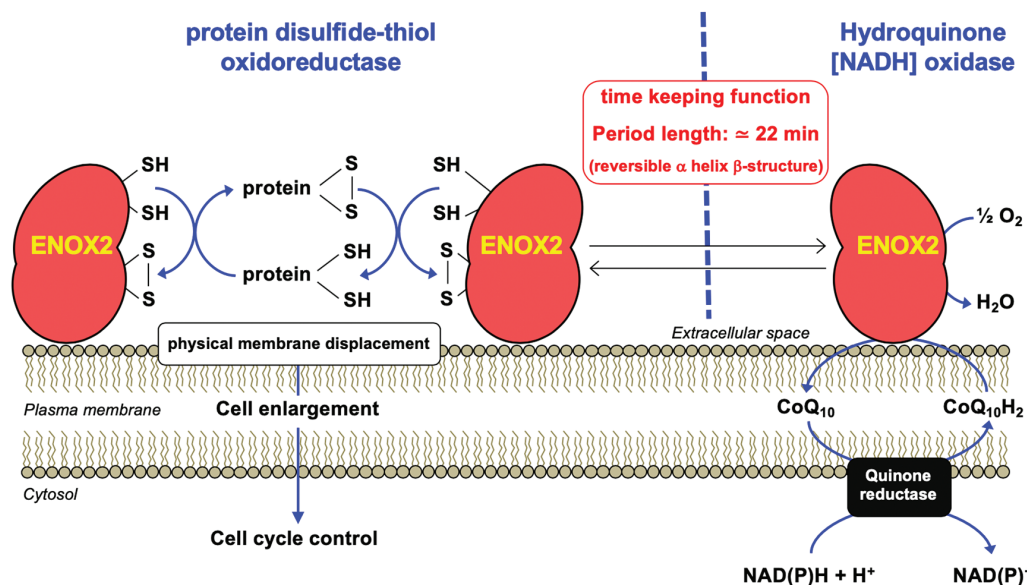
Supplementary Table S2. Continued.					
Gene symbol	R value	p-value	Gene symbol	R value	p-value
FOXE1	0.86260194	<1.0e-6	NR5A1	0.8442461	<1.0e-6
PEMT	0.8624352	<1.0e-6	B3GALT4	0.843811	<1.0e-6
FBXL8	0.8623713	<1.0e-6	PCDHGC5	0.8437889	<1.0e-6
TFF2	0.8621231	<1.0e-6	PDZD4	0.84360224	<1.0e-6
PTCD1	0.86208713	<1.0e-6	RIN3	0.8435184	<1.0e-6
SLC29A3	0.86157095	<1.0e-6	WNK4	0.8434865	<1.0e-6
CHRNA2	0.8613419	<1.0e-6	FBLN1	0.84334964	<1.0e-6
WFDC2	0.8609538	<1.0e-6	ALPP	0.8427555	<1.0e-6
B4GALNT1	0.8607964	<1.0e-6	KCNN1	0.842419	<1.0e-6
ATAD4	0.8601189	<1.0e-6	PTPRU	0.8424166	<1.0e-6
PLK1	0.85977006	<1.0e-6	DKFZP434I0714	0.84233415	<1.0e-6
MSLN	0.8595884	<1.0e-6	LMX1B	0.84229946	<1.0e-6
EPHA1	0.8593882	<1.0e-6	OPTC	0.8420299	<1.0e-6
PAX8	0.859387	<1.0e-6	FIBCD1	0.8418452	<1.0e-6
MTA2	0.8590291	<1.0e-6	FLJ46321	0.84169245	<1.0e-6
FLJ44968	0.8589778	<1.0e-6	RENBP	0.8415789	<1.0e-6
TLL6	0.8582699	<1.0e-6	CLPTM1	0.8406547	<1.0e-6
KRT31	0.8579513	<1.0e-6	ATXN8OS	0.8405387	<1.0e-6
SLC6A12	0.8573194	<1.0e-6	MAZ	0.840483	<1.0e-6
MSI1	0.8559213	<1.0e-6	AGR1	0.8401711	<1.0e-6
ACVR1B	0.85500836	<1.0e-6	PYCR2	0.8400439	<1.0e-6
MYL6	0.8547956	<1.0e-6	MTP18	0.8400094	<1.0e-6
LRRC28	0.85479534	<1.0e-6	SCN2B	0.8394415	<1.0e-6
DESI	0.8547377	<1.0e-6	C1orf172	0.83909196	<1.0e-6
G6PC	0.8529736	<1.0e-6	KRT8P12	0.8378492	<1.0e-6
STARD3	0.8520861	<1.0e-6	ZYX	0.83781403	<1.0e-6
TGM4	0.85199827	<1.0e-6	REG1B	0.8373963	<1.0e-6
C19orf19	0.8512535	<1.0e-6	PCDHGC4	0.83730096	<1.0e-6
PRSS16	0.8508587	<1.0e-6	CST2	0.83702946	<1.0e-6
GPX5	0.85071474	<1.0e-6	RAPSN	0.8365893	<1.0e-6
DRD2	0.8501521	<1.0e-6	COL4A1	0.8365255	<1.0e-6
CALY	0.84971577	<1.0e-6	KIR2DL3	0.8361879	<1.0e-6
UGT1A1	0.848902	<1.0e-6	CRTC1	0.8360285	<1.0e-6
PLEKHA4	0.8486737	<1.0e-6	RNF26	0.83564883	<1.0e-6
EHD2	0.84846425	<1.0e-6	C11orf68	0.835429	<1.0e-6
CCNJL	0.848365	<1.0e-6	ADRA2A	0.83541036	<1.0e-6
C1orf189	0.8483349	<1.0e-6	RFX1	0.83540446	<1.0e-6
CD22	0.84821826	<1.0e-6	MAPK3	0.8353626	<1.0e-6
CYP2D6	0.84755015	<1.0e-6	OR1F1	0.83532614	<1.0e-6
CPAMD8	0.8473105	<1.0e-6	ITIH4	0.834977	<1.0e-6
VPS4B	0.8468782	<1.0e-6	LOC100127937	0.8348357	<1.0e-6
MLH3	0.8464334	<1.0e-6	KCNJ11	0.83476764	<1.0e-6
MAP1S	0.84611046	<1.0e-6	IGSF8	0.8346403	<1.0e-6
MMP17	0.84597486	<1.0e-6	AP1M2	0.83272463	<1.0e-6
GNAO1	0.8455387	<1.0e-6	ZIM2	0.83234274	<1.0e-6
PPP2R4	0.84523815	<1.0e-6	C14orf129	0.8323396	<1.0e-6
ADAM11	0.8447383	<1.0e-6	TAAR5	0.8322871	<1.0e-6

Supplementary Table S2. Continued.					
Gene symbol	R value	p-value	Gene symbol	R value	p-value
<i>XPNPEP3</i>	0.8322395	<1.0e-6	<i>SLC4A2</i>	0.821128	<1.0e-6
<i>C8orf73</i>	0.8317661	<1.0e-6	<i>ECE2</i>	0.8203133	<1.0e-6
<i>RNF151</i>	0.8317153	<1.0e-6	<i>ADAM33</i>	0.8196176	<1.0e-6
<i>COL16A1</i>	0.8315634	<1.0e-6	<i>RCN3</i>	0.8193855	<1.0e-6
<i>SYDE1</i>	0.83143365	<1.0e-6	<i>C8orf4</i>	0.81904936	<1.0e-6
<i>KIFC3</i>	0.83120286	<1.0e-6	<i>GARNL1</i>	0.8188982	<1.0e-6
<i>HDAC10</i>	0.8310805	<1.0e-6	<i>PTMS</i>	0.8184042	<1.0e-6
<i>ZFR</i>	0.830925	<1.0e-6	<i>CARM1</i>	0.81809825	<1.0e-6
<i>CNOT3</i>	0.8305889	<1.0e-6	<i>RGL1</i>	0.8180456	<1.0e-6
<i>COPE</i>	0.8305486	<1.0e-6	<i>PNMAL2</i>	0.8178215	<1.0e-6
<i>TNFRSF12A</i>	0.83052605	<1.0e-6	<i>DYNC2LI1</i>	0.8177664	<1.0e-6
<i>MCOLN1</i>	0.8302164	<1.0e-6	<i>LDB1</i>	0.8173905	<1.0e-6
<i>SHISA5</i>	0.8302118	<1.0e-6	<i>SDS</i>	0.81736207	<1.0e-6
<i>RGS20</i>	0.8301142	<1.0e-6	<i>RBM4</i>	0.8173064	<1.0e-6
<i>LOC100129850</i>	0.82973224	<1.0e-6	<i>WBSCR17</i>	0.8171683	<1.0e-6
<i>GLTSCR1</i>	0.82956636	<1.0e-6	<i>TNN</i>	0.81709546	<1.0e-6
<i>VSTM2L</i>	0.8294069	<1.0e-6	<i>ACTN4</i>	0.8161465	<1.0e-6
<i>SATB1</i>	0.8293123	<1.0e-6	<i>TUB</i>	0.8161079	<1.0e-6
<i>SPRR2D</i>	0.82926977	<1.0e-6	<i>H1FNT</i>	0.81576854	<1.0e-6
<i>CYP11B1</i>	0.8287602	<1.0e-6	<i>CSF2RB</i>	0.815587	<1.0e-6
<i>SGTA</i>	0.8287286	<1.0e-6	<i>CDH23</i>	0.8152525	<1.0e-6
<i>SPRR1B</i>	0.82871044	<1.0e-6	<i>EIF3K</i>	0.81524795	<1.0e-6
<i>SNCB</i>	0.8284577	<1.0e-6	<i>GMEB2</i>	0.81287766	<1.0e-6
<i>APLN</i>	0.8283668	<1.0e-6	<i>ELFN2</i>	0.81287444	<1.0e-6
<i>SPRR2A</i>	0.8283278	<1.0e-6	<i>C14orf172</i>	0.812803	<1.0e-6
<i>RHOG</i>	0.82828736	<1.0e-6	<i>BCL2L2</i>	0.8126579	<1.0e-6
<i>CHAC1</i>	0.82824093	<1.0e-6	<i>DNAJA2</i>	0.81254673	<1.0e-6
<i>TTC22</i>	0.8280334	<1.0e-6	<i>DLK1</i>	0.8124666	<1.0e-6
<i>RNF128</i>	0.82753456	<1.0e-6	<i>ADAM29</i>	0.8123947	<1.0e-6
<i>SNX26</i>	0.82713646	<1.0e-6	<i>MAPK8IP2</i>	0.8121275	<1.0e-6
<i>KIAA1754L</i>	0.82613075	<1.0e-6	<i>FOSL2</i>	0.81212395	<1.0e-6
<i>KIAA1529</i>	0.82609916	<1.0e-6	<i>RAC2</i>	0.8118523	<1.0e-6
<i>RIC8B</i>	0.825819	<1.0e-6	<i>EPB41</i>	0.81175447	<1.0e-6
<i>GNAT1</i>	0.8257777	<1.0e-6	<i>NINJ1</i>	0.81159925	<1.0e-6
<i>SFTPB</i>	0.8254168	<1.0e-6	<i>LOC150837</i>	0.8113656	<1.0e-6
<i>CACNA1F</i>	0.8245132	<1.0e-6	<i>ZDHHC1</i>	0.8102412	<1.0e-6
<i>PI15</i>	0.82392	<1.0e-6	<i>ATP1B4</i>	0.8100232	<1.0e-6
<i>MEGF6</i>	0.8238893	<1.0e-6	<i>GHSR</i>	0.8099814	<1.0e-6
<i>ANKDD1A</i>	0.8237899	<1.0e-6	<i>IL22RA1</i>	0.80987364	<1.0e-6
<i>ITGBL1</i>	0.8236786	<1.0e-6	<i>CABIN1</i>	0.80941373	<1.0e-6
<i>PDK2</i>	0.8232525	<1.0e-6	<i>NPBWR2</i>	0.8083389	<1.0e-6
<i>LMBR1L</i>	0.8232194	<1.0e-6	<i>REG1A</i>	0.8082004	<1.0e-6
<i>FTCD</i>	0.82304573	<1.0e-6	<i>CACNA1A</i>	0.8077839	<1.0e-6
<i>ADRM1</i>	0.822709	<1.0e-6	<i>SLC30A3</i>	0.80736727	<1.0e-6
<i>ARSA</i>	0.8220143	<1.0e-6	<i>MCF2L</i>	0.8068927	<1.0e-6
<i>CYP4A11</i>	0.82194686	<1.0e-6	<i>TCL6</i>	0.80667216	<1.0e-6
<i>IKBKG</i>	0.8217774	<1.0e-6	<i>METTL10</i>	0.8066095	<1.0e-6

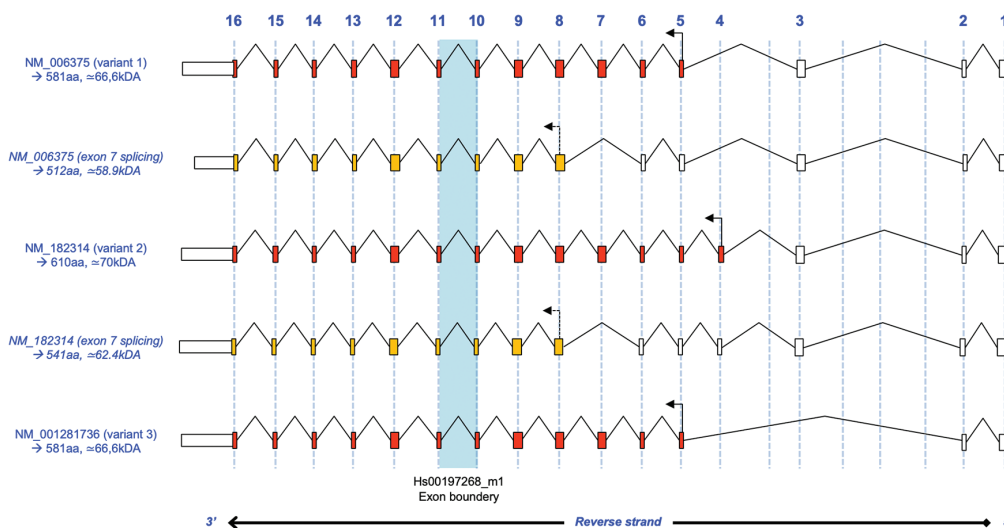
Supplementary Table S2. Continued.		
Gene symbol	R value	p-value
<i>SMAD5OS</i>	0.8059775	<1.0e-6
<i>TC2CD2L</i>	0.8056723	<1.0e-6
<i>RRAS</i>	0.8054051	<1.0e-6
<i>UPB1</i>	0.8044197	<1.0e-6
<i>NPAS1</i>	0.80421555	<1.0e-6
<i>C9orf114</i>	0.8039769	<1.0e-6
<i>RUSC2</i>	0.80360794	<1.0e-6
<i>FASTK</i>	0.8034226	<1.0e-6
<i>HEYL</i>	0.8029919	<1.0e-6
<i>SMR3A</i>	0.8029302	<1.0e-6
<i>THY1</i>	0.80260617	<1.0e-6
<i>IGHMBP2</i>	0.80242604	<1.0e-6
<i>GCK</i>	0.80231726	<1.0e-6
<i>HARS</i>	0.80198824	<1.0e-6
<i>ZMIZ2</i>	0.8013899	<1.0e-6
<i>AP2A2</i>	0.80138415	<1.0e-6
<i>KCNAB2</i>	0.8012798	<1.0e-6
<i>C1QL1</i>	0.80122924	<1.0e-6
<i>VAPB</i>	0.80119395	<1.0e-6
<i>KIAA1688</i>	0.80085427	<1.0e-6
<i>AVPR2</i>	0.800773	<1.0e-6
<i>PSG4</i>	0.8007616	<1.0e-6
<i>LOC400236</i>	0.800309	<1.0e-6
<i>MVD</i>	0.8002809	<1.0e-6

Supplementary Table S3. Proteins of ENOX2 potential network involved in critical biological processes.			
Protein symbol	Complete name	Molecular function	Biological process
ADAM11	ADAM metallopeptidase domain 11	Metallopeptidase activity	Protein metabolism
ADAM33	ADAM metallopeptidase domain 33	Metallopeptidase activity	Protein metabolism
ADRA2A	Alpha 2A adrenergic receptor	G-protein coupled receptor activity	Cell communication; Signal transduction
APLN	Apelin	Receptor binding	Cell communication; Signal transduction
AVPR2	Arginine vasopressin receptor 2	G-protein coupled receptor activity Cell communication; Signal transduction	Cell communication; Signal transduction
BMP7	Bone morphogenetic protein 7	Receptor binding	Cell communication; Signal transduction
CARM1	Coactivator associated arginine methyltransferase 1	Methyltransferase activity	Metabolism; Energy pathways
CHRNA2	Cholinergic receptor, neuronal nicotinic, beta polypeptide 2	Extracellular ligand-gated ion channel activity	Transport
COL16A1	Collagen, type XVI, alpha 1	Extracellular matrix structural constituent	Cell growth and/or maintenance
COL4A1	Collagen, type IV, alpha 1	Extracellular matrix structural constituent	Cell growth and/or maintenance
CYP11B1	Cytochrome P450, subfamily XIB, polypeptide 1	Catalytic activity	Metabolism; Energy pathways
DHPS	Deoxyhypusine synthase	Transferase activity	Metabolism; Energy pathways
DNAJA2 (HIRIP4)	DnaJ heat shock protein family (Hsp40) Member A2 (HIRA interacting protein 4)	Chaperone activity	Protein metabolism
DRD2	Dopamine receptor D2	G-protein coupled receptor activity	Cell communication; Signal transduction
DTX3	Deltex 3	Ubiquitin-specific protease activity	Protein metabolism
EPHA1	EPH receptor A1	Transmembrane receptor protein tyrosine kinase activity	Cell communication; Signal transduction
EPHB3	EPH receptor B3	Transmembrane receptor protein tyrosine kinase activity	Cell communication; Signal transduction
FOSL2 (FRA2)	AP-1 transcription factor subunit (Fos-related antigen 2)	Transcription factor activity	Regulation of nucleobase, nucleoside, nucleotide, and nucleic acid metabolism
G6PC	Glucose-6-phosphatase	Hydrolase activity	Metabolism; Energy pathways
GCK	Glucokinase	Phosphorylase activity	Metabolism; Energy pathways
HEYL	Hairy/enhancer-of-split related with YRPW motif-like	Transcription regulator activity	Regulation of nucleobase, nucleoside, nucleotide, and nucleic acid metabolism
HOXC10	Homeobox C10	Transcription factor activity	Regulation of nucleobase, nucleoside, nucleotide, and nucleic acid metabolism
IKBKG	Inhibitor of kappa light polypeptide gene enhancer in B-cells, kinase gamma	Receptor signaling complex scaffold activity	Cell communication; Signal transduction
ITGBL1	Integrin beta like 1	Cell adhesion molecule activity	Biological process unknown
JAG2	Jagged 2	Receptor binding	Cell communication; Signal transduction

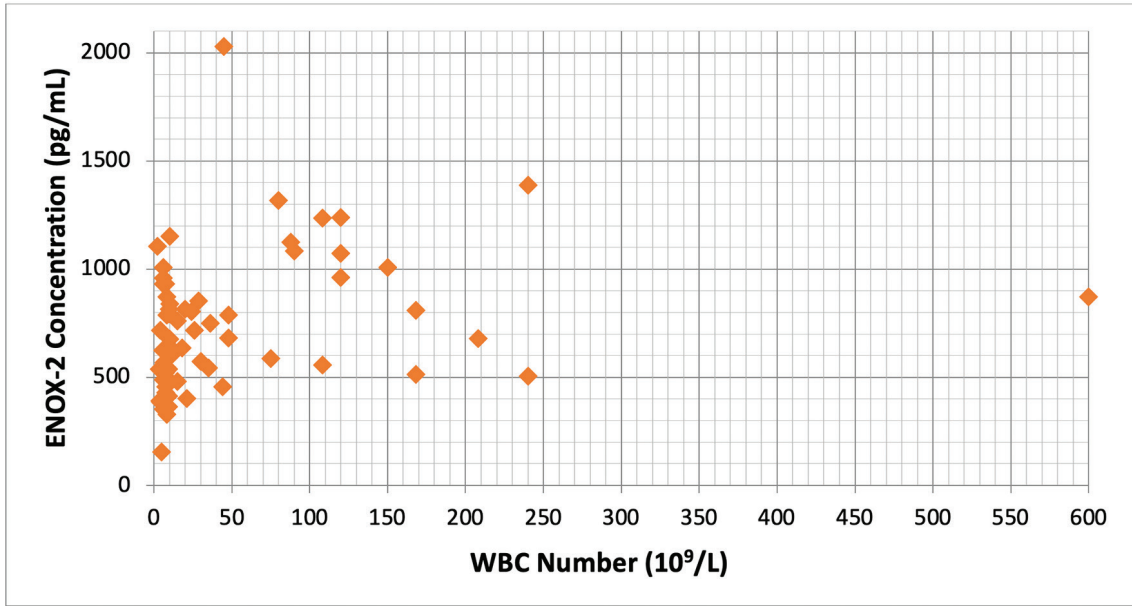
Supplementary Table S3. Continued.			
Protein symbol	Complete name	Molecular function	Biological process
MAPK11	Mitogen-activated protein kinase 11	Protein serine/threonine kinase activity	Cell communication; Signal transduction
MAPK3 (ERK1)	Mitogen-activated protein kinase 3 (Extracellular signal-regulated kinase 1)	Protein serine/threonine kinase activity	Cell communication; Signal transduction
MAPK8IP2 (JIP2)	Mitogen-activated protein kinase 8 Interacting protein 2 (JNK interacting protein 2)	Receptor signaling complex scaffold activity	Cell communication; Signal transduction
MCF2L	Guanine nucleotide exchange factor DBS	Guanyl-nucleotide exchange factor activity	Cell communication; Signal transduction
MVD	Mevalonate pyrophosphate decarboxylase	Carboxy-lyase activity	Metabolism; Energy pathways
PAX8	Paired box 8	Transcription regulator activity	Regulation of nucleobase, nucleoside, nucleotide, and nucleic acid metabolism
PGF (PLGF)	Placental growth factor	Growth factor activity	Cell communication; Signal transduction
PLXDC1 (TEM7)	Plexin domain containing 1 (Tumor endothelial marker 7)	Tumor endothelial marker 7	Cell communication; Signal transduction
PTK2 (FAK)	Protein tyrosine kinase 2 (Focal adhesion kinase)	Protein-tyrosine kinase activity	Cell communication; Signal transduction
RAC2	Ras-related C3 botulinum toxin substrate 2	GTPase activity	Cell communication; Signal transduction
RBM4	RNA binding motif protein 4	RNA binding	Regulation of nucleobase, nucleoside, nucleotide, and nucleic acid metabolism
REG1A	Regenerating family member 1 alpha	Extracellular matrix structural constituent	Cell growth and/or maintenance
RGS20	Regulator of G protein signaling 20	GTPase activator activity	Cell communication; Signal transduction
RGS7	Regulator of G protein signaling 7	GTPase activator activity	Cell communication; Signal transduction
RHOG	Ras homolog family member G	GTPase activity	Cell communication; Signal transduction
RIC8B	RIC8 guanine nucleotide exchange factor B (Brain synembryn)	Guanyl-nucleotide exchange factor activity	Cell communication; Signal transduction
RRAS	Ras-related protein	GTPase activity	Cell communication; Signal transduction
SFTPB	Surfactant protein B	Molecular function unknown	Cellular defense response
SLC2A4	Solute carrier family 2 member 4	Transporter activity	Transport
SYDE1	Synapse defective 1, Rho GTPase, homolog 1	GTPase activator activity	Cell communication
TFAP2B	Transcription factor AP-2 beta	Transcription factor activity	Regulation of nucleobase, nucleoside, nucleotide, and nucleic acid metabolism
THY1	Thy-1 cell surface antigen	Molecular function unknown	Immune response
TNFRSF12A (TWEAKR)	TNF receptor superfamily member 12A (TWEAK receptor)	Receptor activity	Cell communication; Signal transduction
TRIB1	Tribbles homolog 1	Protein threonine/tyrosine kinase activity	Cell communication; Signal transduction



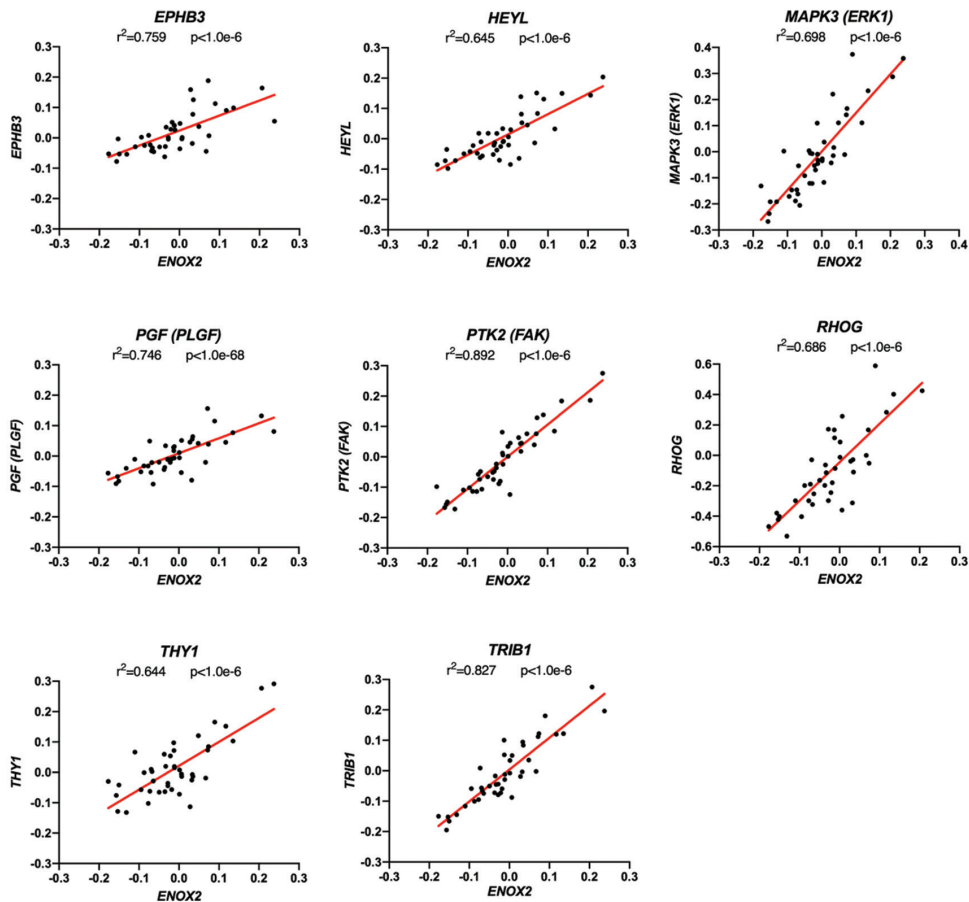
Supplementary Figure S1. Schematic representation of ENOX2 dimer functions at the plasma membrane of a cancer cell. ENOX2 combines two main enzymatic oscillatory activities (hydroquinone NADH oxidase and protein disulfide-thiol oxidoreductase) that alternate with a period length of approximately 22 minutes, generating an ultradian cellular biological clock of 22 hours. Figure from Morrè DJ, Morrè DM. ECTO-NOX Proteins, Growth, Cancer, and Aging. New York, Springer, 2013.



Supplementary Figure S2. Schematic representation of some mature transcript types and alternative splicing observed in ENOX2 gene. Data are from REFSEQ mRNAs (NM_182314 was taken as the reference for exon numbering). The blue bar represents exon 10-11 boundaries for qRT-PCR experiments using ENOX2 TaqMan pre-developed assay reagent (Hs00197268_m1). Theoretically derived molecular weights of proteins translated from the open reading frame of different mRNA isoforms are given as indications. Exons in red and orange correspond to full-length cDNA and exons potentially translated in the case of skipping of exon 7 (alternative translation initiation sites), respectively.



Supplementary Figure S3. No correlation was found between ENOX2 protein levels in the plasma and white blood cell (WBC) count at diagnosis.



Supplementary Figure S4. Several potentially relevant protein-coding genes displaying mRNA expressions significantly correlated with ENOX2 mRNA expression. Linear regression revealed high positive correlation degrees between ENOX2 and EPHB3, HEYL, ERK1, PIGF, FAK, RHOG, THY1, and TRIB1 gene mRNA expression. The r^2 and p parameters are shown on each graph.